

Effect of glass-fibre reinforcement and annealing on microstructure and mechanical behaviour of nylon 6,6

Part I *Microstructure and morphology*

M. L. SHIAO, S. V. NAIR

Department of Mechanical Engineering, University of Massachusetts, Amherst, MA 01003, USA

P. D. GARRETT, R. E. POLLARD,

Monsanto Chemical Co., Springfield, MA 01151, USA

The effects of glass fibres and annealing on the microstructures and spherulitic morphology of a glass fibre-reinforced nylon 6,6 were investigated. The annealing effects on matrix crystallinity of nylon 6,6 composites with varying glass fibre contents were measured and the morphology of the composites were examined using both the microtomed bulk samples and thin composite films prepared by melt crystallization. It was found that fibre breakage during injection moulding was significant for composites with glass content higher than 20 wt%, and the spherulite size as well as the crystallinity were reduced by the additions of glass fibres. Upon annealing, the start of a log time rate increase of matrix crystallinity was delayed by the addition of glass fibres. Glass fibre-induced transcrystallinity was not observed in injection-moulded composites; however, columnar spherulites were found to develop along the glass fibres in melt-crystallized thin composite films. Differences in morphological observations between the two sample preparation methods are also discussed.

1. Introduction

Semi-crystalline polymers, such as nylon 6,6 have been extensively used in many engineering applications owing to their outstanding mechanical properties and relative ease of fabrication [1–3]. At the molecular level these polymers generally consist of unoriented spherulites within which crystallites, known as lamellae, grow radially from its nucleus and are separated by amorphous layers connected by tie molecules [4]. Microstructural features, e.g. size and morphology of spherulites and degree of crystallinity, are known to influence strongly the material's mechanical properties [4–7]. These microstructural features and, in turn, the physical and mechanical properties, are also sensitive to annealing of the polymer [6, 8, 9] as well as to the presence of second-phase reinforcements [10–13] as in fibre-reinforced semi-crystalline polymers.

The influence of annealing on the crystalline microstructure and mechanical properties has been previously examined [8, 9, 14–17]. There have also been many studies [11, 18–22] on the influence of glass fibres on mechanical properties, with more limited studies [10, 12, 13, 23] on how glass fibres affect the crystalline microstructure and crystallization rate of the base polymers. The formation of columnar spherulites known as transcrystallinity has been observed through heterogeneous nucleation along the glass fibre-matrix interfaces [24]. Recently, it has also been

reported that the glass fibres, as well as the amount added, can increase the crystallization rate and consequently affect the microstructure of the base polymers [25]. However, there has yet to be a systematic study on the combined effects of glass fibres and annealing on the crystalline microstructure and mechanical properties of nylon 6,6 composites.

In this paper, the microstructure and morphological aspects of nylon 6,6 composites due to increasing glass fibre content and annealing will be reported. In Part II of this study [26] the corresponding influence of glass fibres and annealing on the deformation and fracture mechanisms of the composites will be addressed.

2. Experimental procedure

2.1. Materials

The materials studied were glass fibre-reinforced poly(hexamethylene adipamide), or nylon 6,6. The composites were made by dry blending of chopped E-glass fibres and were injection moulded. The chopped E-glass fibres were nominally 13 μm diameter and were about 4 mm long prior to injection moulding. Seven loading levels of glass fibre reinforcement, 0%, 1%, 5%, 10%, 20%, 30% and 40% by weight of the matrix, were made to examine systematically the role of glass fibres. To avoid moisture and light degradation effects, after injection moulding the specimens

were sealed first in PE film and then in aluminized paper until they were tested.

2.2. Annealing and crystallinity determination

The role of crystallinity in the materials was studied through annealing of the specimens. Three sets of samples, the unreinforced nylon 6,6, 10 wt % and 30 wt % glass-filled composites, were used to investigate the effect of annealing. All annealing was carried out in vacuum at 150 °C for various annealing times. After the desired annealing time, the specimens were cooled slowly in vacuum to room temperature. Upon removal of the specimens from the oven they were then stored in moisture-proof bags for 24 h prior to testing.

The degree of crystallinity, both in the unreinforced and in the composite materials, was determined by measurements of specimen density using a density gradient column (ASTM D1505). The density column was constructed using toluene and carbon tetrachloride with a density range of 0.99–1.40 g cm⁻³ and with an accuracy of 0.0004 g cm⁻³ mm. Three density samples for each annealing condition were sliced by taking transverse cross-sections of the bulk injection-moulded specimens to obtain an average density of the materials. In the unreinforced nylon 6,6 the percent crystallinity was directly calculated using known density data for nylon 6,6 namely, an amorphous density $d_a = 1.091 \text{ g cm}^{-3}$ and 100% crystalline density of $d_c = 1.241 \text{ g cm}^{-3}$ [27].

In the case of the composites, the matrix density and hence the matrix crystallinity were determined from density measurements of the composites using the relation

$$D_c = \left(\frac{f_g}{D_f} + \frac{1-f_g}{D_m} + \frac{x}{D_c} \right)^{-1} \quad (1)$$

or

$$D_m = \frac{D_c D_f (1 - f_g)}{D_f (1 - x) - D_c f_g} \quad (2)$$

where D_c , D_m individually represent the density of the composite and the matrix density of the composite; D_f is the measured density of glass fibre with coupling agent, and f_g are the weight fraction of glass fibres and the volume fraction of voids, respectively. D_f was measured to be 2.5314 g cm⁻³. Thus by measuring the density of the composites, one can then calculate the matrix density and hence the matrix crystallinity of the composites from Equation 2. In this study, the influence of void volume fraction, x , in Equation 2 was found to be negligible [28] and for simplicity it was neglected in the calculations.

2.3. Microstructure

The microstructures of the composites were revealed by optical microscopy using an Olympus AH-2 microscope on surfaces of the specimens polished to a 1 μm diamond finish. The microstructures were only examined at the central region of the injection-moulded

specimens in order to minimize the effects of mould geometry on fibre orientations.

The average glass fibre lengths were measured using the lineal analysis method [29] on micrographs of extracted glass fibres from composite samples. Two random lines were drawn across the micrographs to be examined. Each glass fibre intersected by the lines was counted and its length was measured (accuracy ± 20 μm). The same procedure was carried out on composites with glass fibre loading levels of 10, 20, 30 and 40 wt %. The standard deviation was estimated to be less than 10 μm by measurements on different micrographs of extracted glass fibres from the same 40 wt % glass composites. The image analysis method using an image analyser on the same micrographs of extracted glass fibres proved to be unsatisfactory because longer glass fibres were not counted due to crossing with nearby fibres.

2.4. Morphology

The morphology of the spherulites in the unreinforced and glass fibre-reinforced nylon 6,6 were studied by cross-polarized light microscopy on microtomed thin sections. Approximately 5 μm thick thin films were microtomed from bulk injection moulded specimens. In the case of glass-filled composites, the microtomed samples were obtained by using a carbide blade equipped with a heavy duty blade holder to prevent vibrations during cutting.

Additional morphological investigations on unreinforced and glass fibre-reinforced nylon 6,6 were also carried out by preparing thin film samples using the melt-crystallization method [10]. For this purpose a thin film of nylon 6,6 was first solution cast on a degreased microslide using 5% formic acid solution. After vacuum evaporation of the solvent at 85 °C, chopped E-glass fibres with coupling agent were then placed on the thin film. The thin film with glass fibres was then closed tightly in a small aluminium chamber filled with argon and was subsequently heated in a circulating oven at 295 °C for 5 min for complete melting of nylon 6,6. After melting of the nylon 6,6, the composite thin film was then crystallized at 85 °C for 3 min in a water bath. The temperature profile used in this thin-film preparation was chosen to simulate the temperature cycle during injection moulding. The prepared thin composite films were then examined by cross-polarized light microscopy to investigate the spherulite morphology.

3. Results and discussion

3.1. Microstructure

The microstructures of the glass fibre-reinforced nylon 6,6 are shown in Fig. 1a–f for composites with glass fibre contents of 1, 5, 10, 20, 30 and 40 wt %, respectively. As can be seen in Fig. 1, the dispersion of glass fibres in nylon 6,6 was fairly uniform throughout the whole range of fibre contents studied and also no significant voids or defects along the glass fibres and at fibre ends could be found. As the glass fibre content increased (Fig. 1a–f, increased fibre breakdown could

→ Flow direction

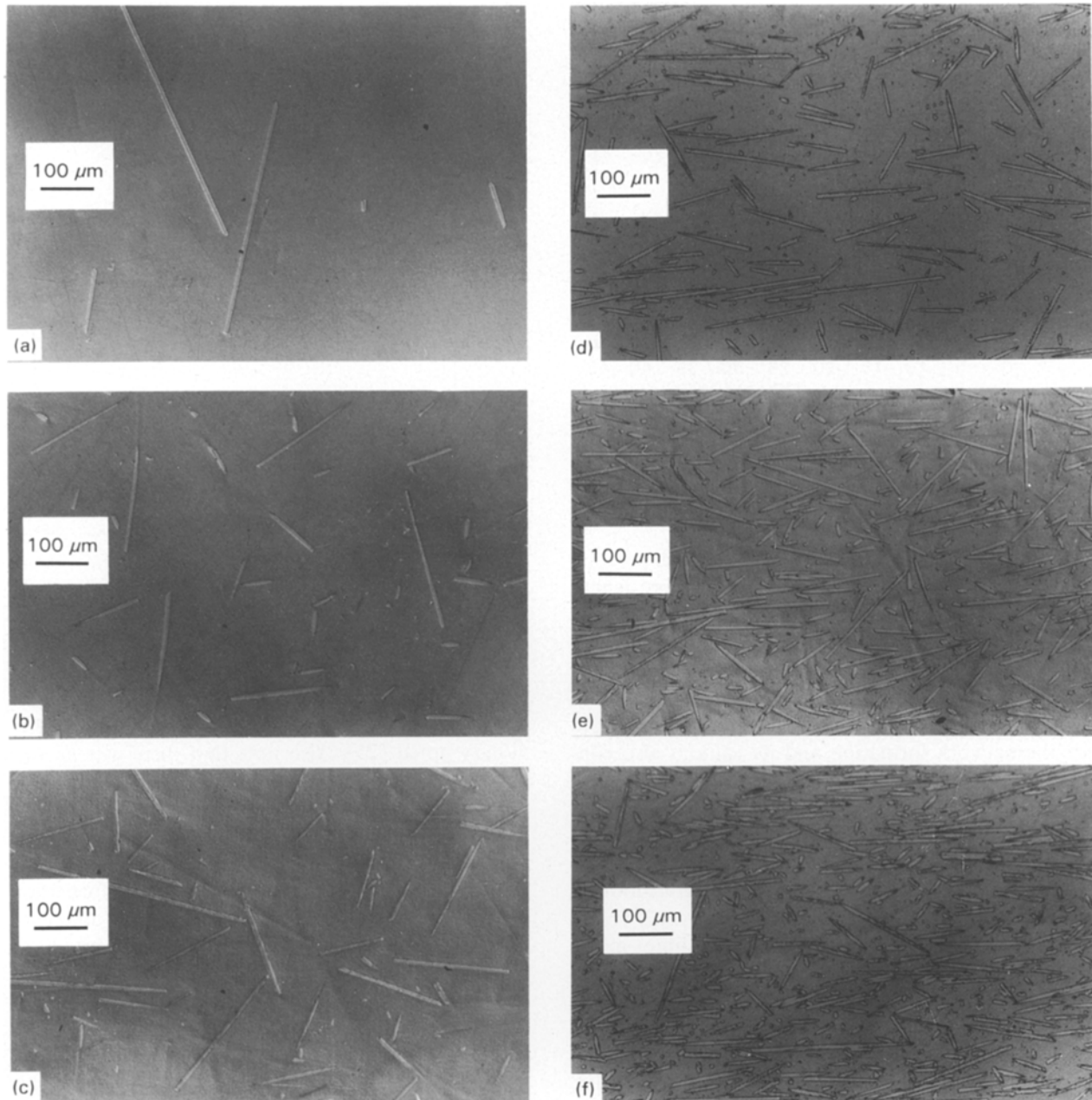


Figure 1 Optical micrographs showing the microstructures of nylon 6,6 composites: (a) 1 wt %, (b) 5 wt %, (c) 10 wt %, (d) 20 wt % (e) 30 wt % and (f) 40 wt % glass-filled composites.

be observed, resulting in a significant volume fraction of glass fibre fragments in the composites of higher glass fibre contents. Consequently, the average fibre length was substantially reduced as the glass fibre content was increased. Such reduction of fibre length due to increasing glass fibre content is shown in Fig. 2, where the average glass fibre length is plotted as a function of glass fibre content. As can be seen in Fig. 2, the reduction of glass fibre length due to fibre breakdown was most severe in the range between 20 and 30 wt % glass content. Further increase of glass fibre content above 30 wt % did not seem to reduce greatly the average fibre length. Because all the composite specimens were injection moulded under the same conditions, it is believed that the increased fibre break-

down was most likely due to increasing geometric constraints imposed by nearby glass fibres during the flow process of injection moulding. Hence the result shown in Fig. 2 implies that fibre breakdown due to geometric constraints by nearby glass fibres was most substantial for composites when the glass fibre content was passed through 20 wt %. This result may be explained on the basis that at a critical volume fraction of glass fibres, the constrained matrix region percolates through the sample allowing for significant fibre breakage. Percolation theory proposes a scaling law that any property, p , of the percolated sample varies as [30]

$$p \propto (f - f_c)^n \quad (3)$$

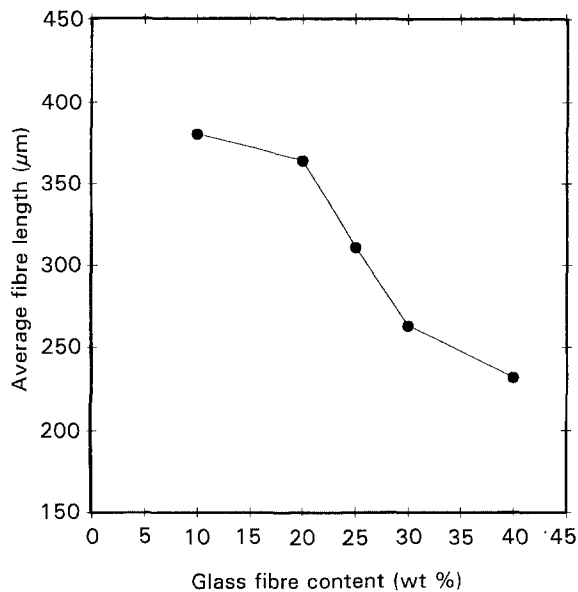


Figure 2 Average fibre length versus glass fibre content in nylon 6,6 composites.

where f_c is the critical concentration at which percolation is achieved. A plot of the average fibre length versus $(f - f_c)^n$ using critical volume fraction $f_c = 0.101$ (equivalent to 20 wt % glass fibres) was found to be consistent with Equation 1, see Fig. 3. The observed critical glass content of 20 wt % (10.1% in volume) can therefore be thought of as the threshold for the network formation and its value is also consistent with other results of studies in conductivity of carbon fibre-reinforced polymers [31, 32]. The exponent, n , was found to be 0.2. As will be seen later in Part II [26], nylon 6,6 composites with glass fibre contents passing through 30 wt % also showed a transition in their mechanical properties.

Also in Fig. 1, the orientation of glass fibres in the centre part of composite specimens with higher glass content (Fig. 1e and f) was found to be more aligned in the flow direction, while in the composites of lower glass content (Fig. 1a and b) the fibre is less oriented. Again this is consistent with the fact mentioned earlier, that in the composites with low glass contents the geometric constraints imposed by nearby fibres within the flow were less significant than those of the composites with high glass contents. Hence the fibre orientation of low glass-containing composites tended to be more random along the flow line than in the composites of high glass contents.

3.2. Morphology

3.2.1. Microtomed specimens

Fig. 4. shows the micrograph of the spherulitic morphology of an unreinforced nylon 6,6 material using cross-polarized light microscopy. As can be seen in Fig. 4a, an amorphous skin layer, about 10–15 µm thick, was observed in the injection-moulded tensile specimens. The spherulite size was found to be approximately 15–20 µm diameter (see Fig. 4b and c).

In the glass fibre-reinforced composites, however, the spherulite size appeared to be much smaller, as

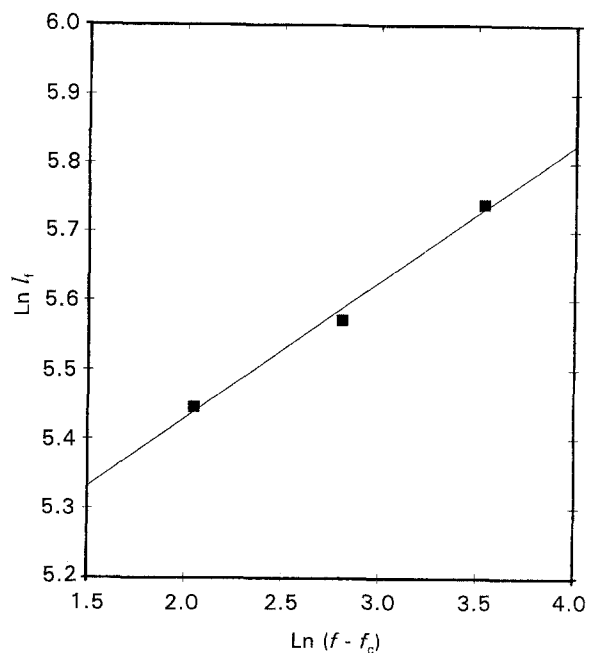


Figure 3 Log-log plot of average fibre length l_f , versus glass fibre content above the critical glass content, f_c , of 20 wt % (equivalent to 0.101 in volume).

shown in Fig. 5. The approximate spherulite size was of the order of 2–5 µm. Similar results of the effects of glass fibre reinforcement on reducing the spherulite size in semi-crystalline polymers have also been previously noted [25]. Also note that there was no evidence of a transcrystalline region along the glass fibre–matrix interfaces (see Fig. 5b and c). Unfortunately, more detailed observation of the spherulitic morphology along the fibre–matrix interfaces was difficult owing to microtome-induced deformation around this region. Because the modulus difference between nylon 6,6 and E-glass fibre is very large (about 1–45), it also becomes progressively difficult to keep the integrity of microtomed composite samples for morphology observation as the glass content increases. Other methods, such as melt crystallization, were thus also used to study the effects of glass fibres on the crystalline morphology of nylon 6,6. They will be discussed in the next section.

3.2.2. Melt-crystallized specimens

Micrographs of the spherulitic morphology in melt crystallized nylon 6,6 are shown in Fig. 6 using cross-polarized light microscopy. The spherulite size appeared to be somewhat larger than the spherulite size in microtomed bulk samples and was of the order of 50 µm. However, note that, by this method, the Maltese cross pattern inside the spherulite structure of nylon 6,6 can be clearly seen, as shown in Fig. 6a. The boundaries between spherulites shown in Fig. 6b can also be clearly seen, except in those spherulitic boundaries where the extinction pattern resulting from lamellae of nearby spherulites were laid in the same direction (see arrow in Fig. 6b). In such cases, the extinction pattern seems to extend through the boundary and meet others in the neighbouring spherulite.

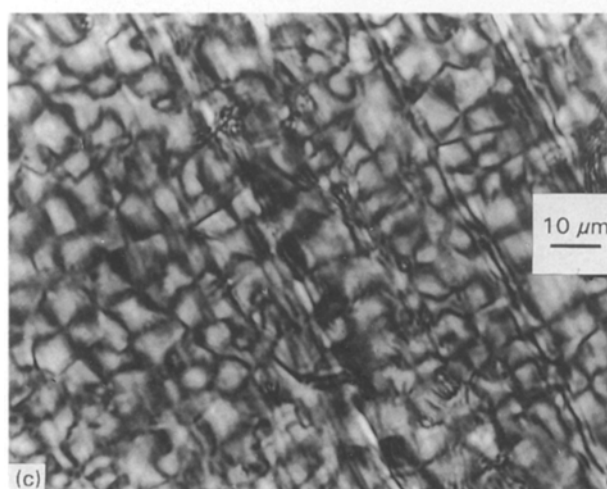
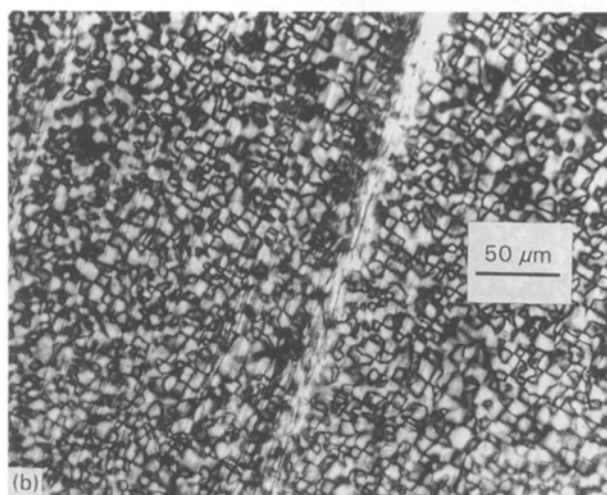
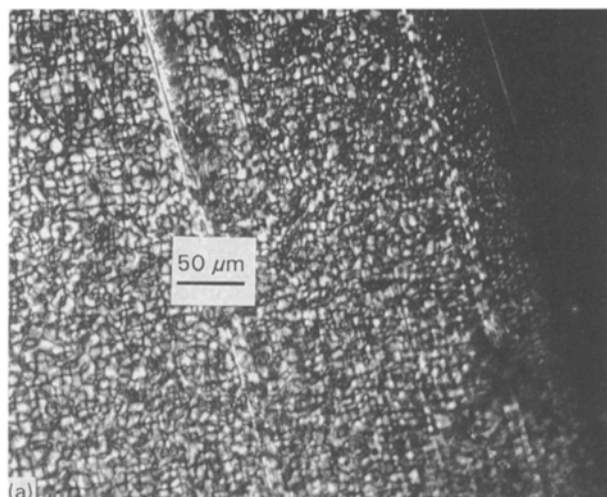


Figure 4 Cross-polarized micrographs of microtomed nylon 6,6 bulk samples. (a) Low magnification; (b, c), higher magnification.

This causes the boundary between spherulites to become less distinct.

In the case of melt-crystallized composite thin films, it was observed that glass fibres can induce columnar spherulites or transcrystalline regions along the fibre–matrix interfaces, as shown in Fig. 7a. However, the existence of such regions was found to be irregular. For instance, the transcrystalline region shown in

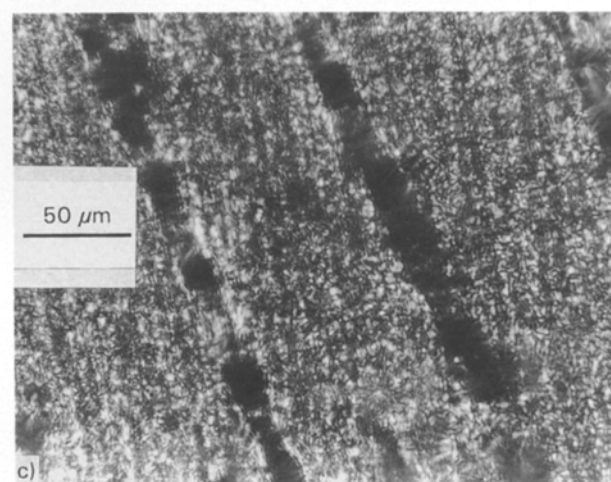
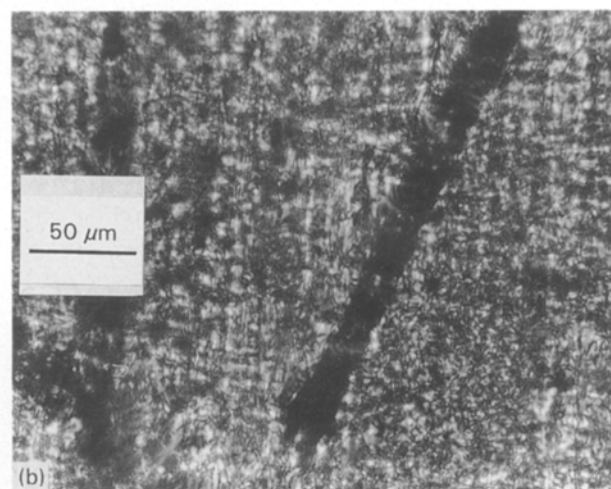
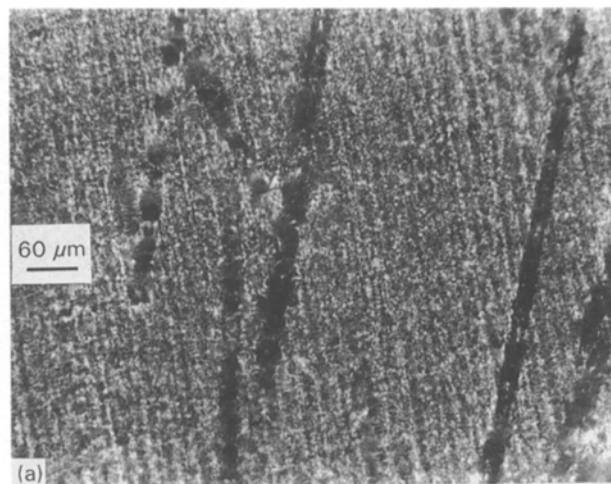


Figure 5 Cross-polarized micrographs of microtomed nylon 6,6 composite containing 10 wt % glass fibres. (a) Low magnification; (b, c) higher magnification.

Fig. 7b did not form completely along the fibre–matrix interface and in other cases (Fig. 7c) it did not even appear, even though it may appear in a nearby glass fibre. Similar results have also been reported by Bessell and Shortfall [10] in studying the interfacial morphology in melt-crystallized nylon 6. They suggested that the irregularity of the transcrystalline region observed may due to non-uniform

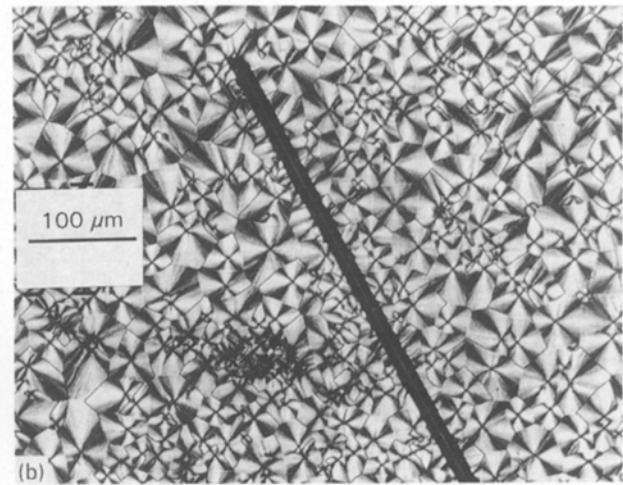
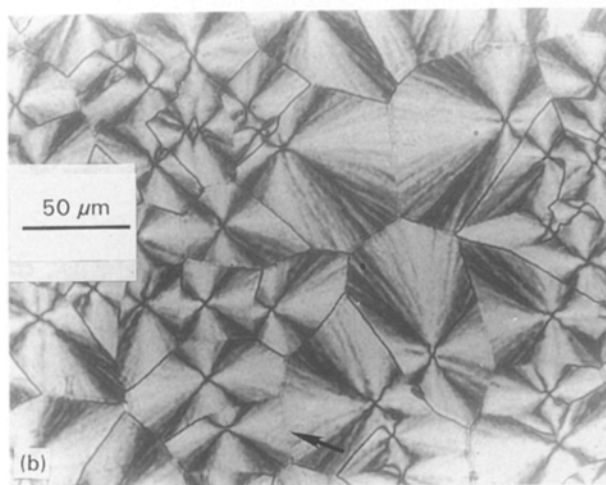
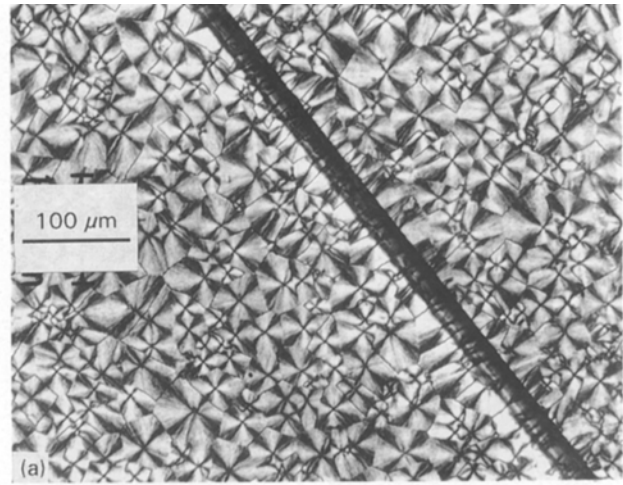
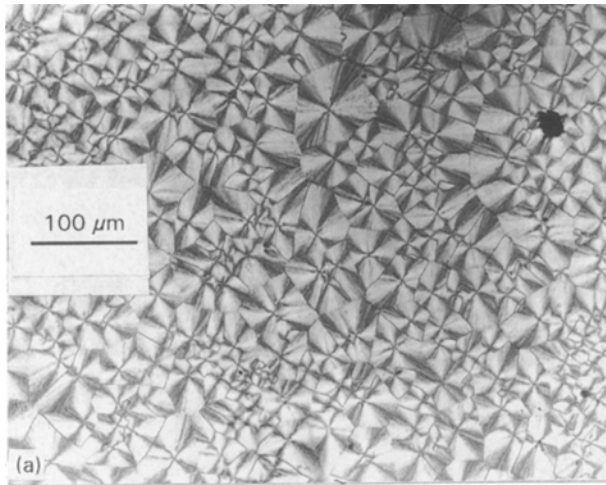


Figure 6 Cross-polarized micrographs showing spherulites in melt-crystallized nylon 6,6 films. (a) Low magnification; (b) higher magnification.

dispersion of organic sizing and also by local dissolution of the sizing which all can enhance the nucleation of the polymer.

Also note that, in Fig. 7, the spherulite size, as compared to the unfilled nylon 6,6 in Fig. 6, was not significantly affected by the presence of glass fibres. It was observed, however, that the spherulite size around the glass fibres was larger only when the glass fibres were very close or clustered together to form fibre bundles (see Fig. 8). This may result from the increased growth rate of spherulites due to additional thermal energy contributed from the glass fibres during the quenching process. The comparison of observations between the microtomed bulk specimens and the melt crystallized specimens will be discussed in Section 3.4.

3.3. Annealing effects

The matrix density, determined through density measurements using Equation 2, versus the corresponding annealing time, is shown in Fig. 9 for the unreinforced, 10 and 30 wt % glass-filled nylon 6,6. Also in Fig. 9, the corresponding scale in matrix crystallinity is shown. As can be seen in Fig. 9, the unreinforced nylon 6,6 had the highest as-moulded density prior to annealing. Increasing the glass fibre content appeared to

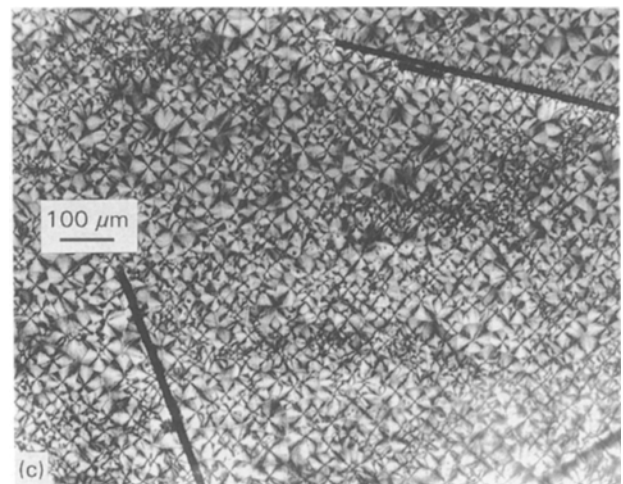


Figure 7 Cross-polarized micrographs showing transcrystallinity in thin films of melt-crystallized nylon 6,6 composites. In (a) the columnar spherulites were well-developed, while in (b) and (c) the lack of uniformity in transcrystallinity can be seen.

reduce slightly the initial as-moulded density or the matrix crystallinity, with lowest initial density for the 30 wt % glass composite. Similar results have also been reported by Reinsch and Rebenfeld [25] in studying the crystallization of fibre-reinforced PET. However, in their case, the decrease in matrix crystallinity was very substantial. Secondly, the glass fibres were also seen to influence the crystallization kinetics during annealing. It is known that melt-crystallized

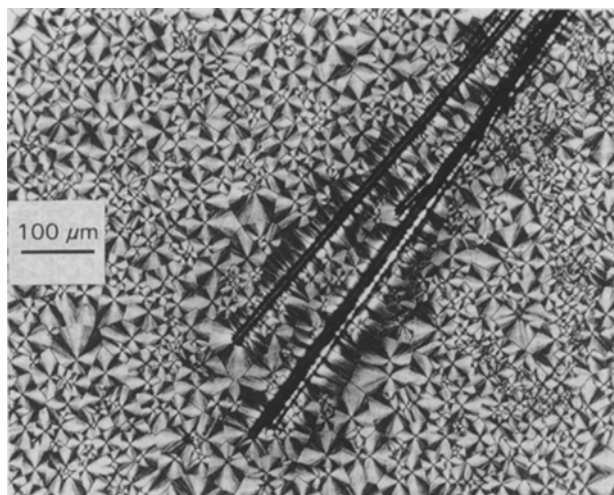


Figure 8 Cross-polarized micrographs showing the effects of glass fibres on the spherulitic morphology in thin films of melt-crystallized nylon 6,6 composites.

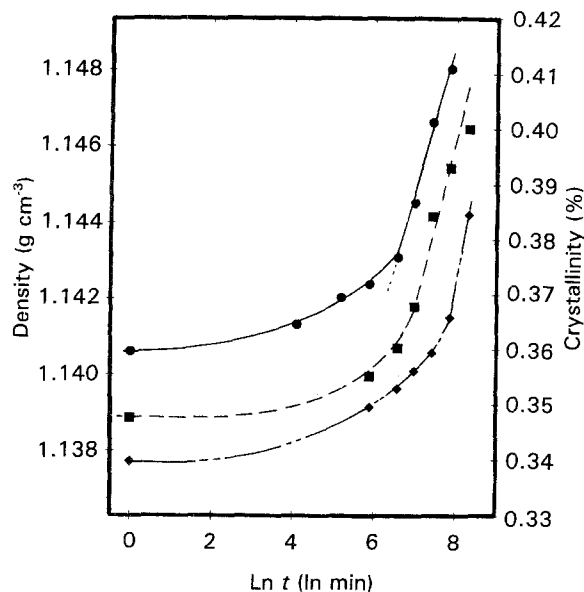


Figure 9 The effects of annealing time on the matrix density of the (●) unreinforced nylon 6,6 (■) 10 and (◆) 30 wt % glass fibre reinforced nylon 6,6 composites.

polymers exhibit a characteristic log time annealing rate [8]. As can be seen in Fig. 9, the start of log time rate behaviour was delayed by the addition of glass fibres.

The increase in the matrix density of nylon 6,6 composites by annealing could be described by the relation

$$\frac{D_m}{D_m^0} = \exp\left(\frac{t - t_0}{\tau}\right) \quad (4)$$

where t is the annealing time; D_m^0 denotes the matrix density at the starting time of annealing, t_0 . τ in the above equation can be regarded as the effective relaxation time which can depend on the molecular mechanisms associated with the process of density increase during annealing. The effective relaxation time, τ , can be obtained from the best fitting of Equation 4 to the

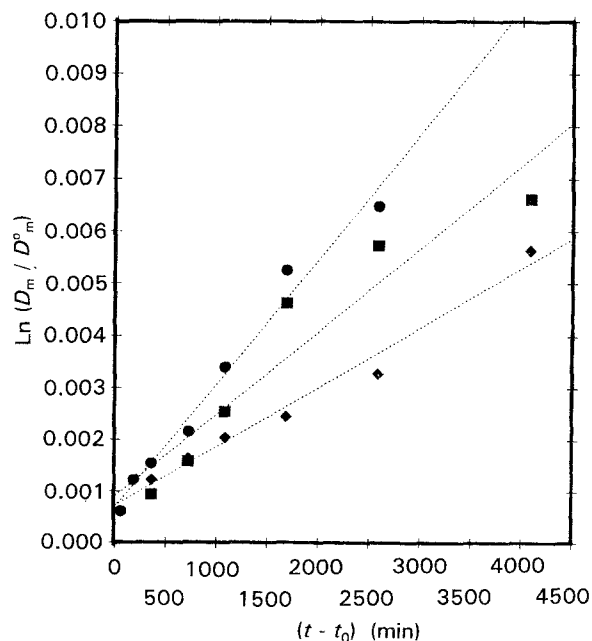


Figure 10 Comparison of annealing data and (----) the prediction of Equation 4. For key, see Fig. 9

TABLE I The calculated effective relaxation time (τ)

Materials	D_m^0	$\tau (\times 10^5 \text{ min})$
Unreinforced nylon 6,6	0.359	4.86
10 wt % glass composite	0.3469	3.32
30 wt % glass composite	0.3391	2.47

experimental data in a log-log plot, as shown in Fig. 10. As can be seen, good agreements between Equation 4 and the experimental data were observed, except in the case of 10 wt % glass composites. Note that the effective relaxation time, τ , was increased as the glass fibre content increased. The calculated effective relaxation time, τ , from Equation 4 are listed in Table I. As can be seen, the addition of up to 30 wt % glass fibres almost doubled the relaxation time, compared to the unreinforced nylon 6,6. This result can be explained by the observation that the molecular mobility of a polymer matrix can be reduced by the addition of glass fibres [33]. It is known that the glass transition temperature, T_g , and the deflection temperature of filled polymers can be significantly increased by increasing the glass fibre contents ([1] p. 387, [33]). Hence, the increase in the relaxation time, or the delay in the start of log time rate as the glass composites were annealed, can be related to the lowering of molecular mobility due to the addition of glass fibres.

3.4. Discussion of microstructural differences between melt-crystallized and microtomed bulk samples

The investigation of spherulite structure along fibre-matrix interfaces has raised some questions regarding the formation of the transcristalline region along interfaces. In the melt-crystallized film samples (Fig. 7) columnar spherulites were found to develop around

the glass fibres, whereas such regions were not observed in the microtomed samples from bulk injection-moulded composites (Fig. 5). It is known that surfaces of fibre reinforcements in semi-crystalline polymers can affect the crystalline morphology by providing nucleation sites for spherulite growth [10, 12, 23–25, 34–37]. Such spherulites grown from the fibre surfaces were often epitaxial, and the extent of such regions was found to be greatly influenced by fibre types and less by fibre surface treatments [10]. For fibre reinforcements which contain crystallites, such as carbon fibre and Kevlar fibre, a pronounced transcrystalline region along the interfaces was often observed [23, 24, 34–37]. The crystallinity in the reinforced fibres has been suggested [34] as a necessary, but not a sufficient, condition for the formation of the transcrystallinity. Other mechanisms, such as crystallographic matching [38] and chemisorption [38] have also been proposed to explain the formation of a large amount of columnar spherulites along the fibres. However, Chatterjee *et al.* [34] have concluded that neither the similarity in chemical structures or crystallographic unit cell, nor a close match of crystal lattice parameters, were necessary for the existence of observed transcrystallinity. More recently, Thomason and Van Rooyen [36] have proposed that the transcrystallization was related to stress-induced nucleation due to the thermal stresses caused by cooling two materials with a large difference in thermal expansion coefficients. They showed that the transcrystallization was dependent on the thermal expansion coefficient of the fibre and on the sample cooling rate, but was independent of the fibre type.

In the case of glass fibres, however, the presence of the transcrystalline region was less noticeable. It has been observed in nylon 6 [10] and nylon 6,6 in this study using the melt-crystallization method, in PP [39] using the hot-stage method, in PET using compression moulding [25], but it was not observed in nylon 6,6 using a hot-stage method [23]. It was also absent in bulk injection-moulded specimens, as shown in this study (see Fig. 5) and by Burton and Folkes [23]. They have also suggested that the absence of such a region in bulk specimens may be due to nucleation effects of fibre debris and residual crystal nuclei from previous thermal history. In our case, the possibility of reducing the transcrystalline region due to nucleation effects by fibre debris seems unlikely, because very little fibre debris could be seen (Figs 3 and 5). In this study, a more significant difference between the melt-crystallized and microtomed bulk samples was in the spherulite sizes, which were about 20 and 5 μm , respectively. It has been shown by Bessell and Shortfall [10] that the transcrystalline region can be substantially reduced by reducing the spherulite size. Hence the absence of interfacial columnar structure in bulk injection-moulded nylon 6,6 composites may result from the significant reduction of spherulite size in the matrix. Also, as been discussed by Thomason and Van Rooyen [36] the appearance of transcrystallinity is dependent on the cooling rate of the material. As the cooling rate increased, the tendency for transcrystallization is also increased by increasing

thermal residual stresses. Because the cooling rate in the thin-film samples studied can be much higher than that in the bulk materials, it is also possible that the transcrystallinity is only observed in the thin composite films due to the cooling rate effect.

Another aspect of morphological difference between the melt-crystallized and microtomed samples was the effect of glass fibres on the overall matrix spherulite size. In the case of microtomed samples the spherulite size was reduced significantly by the addition of glass fibres (see Figs 4 and 5), whereas no appreciable change of spherulite size can be found in melt-crystallized samples (see Figs 6 and 7). The reduction of spherulite size in bulk injection-moulded specimens was most likely due to changes in processing variables with increasing glass fibre content during injection moulding, such as changes in hydrostatic pressure and polymer flow rate, which may vary the melting conditions of the base polymer [41]. Consequently, more residual crystal nuclei from previous thermal history may be left in the matrix of the composites which can act as nucleation agents and thereby result in smaller spherulites during subsequent crystallization. Such effects of glass fibres would not be present in prepared melt-crystallized samples.

4. Conclusions

1. Glass fibre breakage during injection moulding of a nylon 6,6 composite was found to be most severe when the glass fibre content was higher than 20 wt %.

2. The spherulite size in injection-moulded nylon 6,6 was reduced by the addition of glass fibres. The matrix crystallinity of the nylon 6,6 composites was slightly lowered as the glass fibre content was increased.

3. No transcrystallinity at the glass–fibre interfaces was found in the injection-moulded nylon 6,6 composites. The effects of transcrystallinity on the mechanical properties of glass-filled nylon 6,6 would therefore be negligible. However, columnar spherulites were observed to grow along the glass fibres in melt-crystallized nylon 6,6 thin composite films.

4. Upon annealing, the glass fibres were found to delay the start of the log time rate increase of the matrix density. This result may be explained by the reduction in molecular mobility due to the addition of glass fibres.

Acknowledgements

This work was supported by a grant from the Monsanto Chemical Company, Springfield, Massachusetts. Helpful discussions with Dr Robert L. Kruse, Monsanto Chemical Company, are also gratefully acknowledged.

References

1. M. I. KOHAN (ed.), "Nylon Plastics" (Wiley, New York, 1973) p. 1.
2. R. O. CHAPMAN and J. L. CHRUMA, in "Engineering Thermoplastics", edited by J. M. MARGOLIS (Marcel Dekker, New York, 1985) p. 83.

3. W. SWEENEY and J. ZIMMERMAN, in "Encyclopedia of Polymer Science and Engineering", Vol. 11 (Wiley, New York, 1988) p. 315.
4. J. M. SCHULTZ, *Polym. Eng. Sci.* **24** (1984) 770.
5. A. PETERLIN, in "Polymeric Materials", paper presented at a seminar of the American Society for Metals, September 1973, Metals Park, OH (ASM Metals Park, OH, 1975) p. 175.
6. P. B. BOWDEN and R. J. YOUNG, *J. Mater. Sci.* **9** (1974) 2034.
7. J. SCHULTZ, in "Polymer Materials Science" (Prentice Hall, New Jersey, 1974) p. 466.
8. E. W. FISCHER, *Pure Appl. Chem. English Ed.* **31** (1972) 113.
9. H. W. STARKWEATHER JR, G. E. MOORE, J. E. HANSEN, T. M. RODER and R. E. BROOKS, *J. Polym. Sci.* **XXI** (1956) 189.
10. T. BESSELL and J. B. SHORTFALL, *J. Mater. Sci.* **10** (1975) 2035.
11. M. J. FOLKES, in "Short Fiber Reinforced Thermoplastics" (Research Studies Press, Chichester, 1982) Ch. 3.
12. Y. LEE and R. S. PORTER, *Polym. Eng. Sci.* **26** (1986) 633.
13. G. P. DESIO and L. REBENFELD, *J. Appl. Polym. Sci.* **39** (1990) 825.
14. B. WUNDERLICH, in "Macromolecular Physics", Vol. 2 (Academic Press, New York, 1986) Ch. 7.
15. D. P. RUSSELL and P. W. R. BEAUMONT, *J. Mater. Sci.* **15** (1980) 216.
16. G. C. ALFONSO, E. PEDEMONTE and C. PONZETTI, *Polymer* **20** (1979) 104.
17. R. S. SCHOTLAND, *Polym. Eng. Sci.* **6** (1966) 244.
18. W. V. TITOW, B. J. LANHAM, in "Reinforced Thermoplastics" (Applied Science, London, 1975) p. 145.
19. Z. HASHIN, *J. Appl. Mech.* **50** (1983) 481.
20. B. LAUKE, B. SCHULTRICH and W. POMPE, *Polym. Plast. Technol. Eng.* **29** (1990) 607.
21. P. T. CURTIS, M. G. BADER and J. E. BAILEY, *J. Mater. Sci.* **13** (1978) 377.
22. S. V. NAIR, M. L. SHIAO and P. D. GARRETT, *ibid.* **27** (1992) 1085.
23. R. H. BURTON and M. J. FOLKES, *Plast. Rubber Proc. Appl.* **3** (1983) 129.
24. T. BESSELL, D. HULL and J. B. SHORTFALL, *Nature Phys. Sci.* **232** (1971) 127.
25. V. E. REINSCH and L. REBENFELD, in "Proceedings of the ANTEC '91", Montreal, May 1991 (Society of Plastic Engineers, 1991) p. 2075.
26. M. L. SHIAO, S. V. NAIR, P. D. GARRETT and R. E. POLLARD, *J. Mater. Sci.* **29** (1994) 1739.
27. J. P. RUNT, in "Encyclopedia of Polymer Science and Engineering", Vol. 4 (Wiley, New York, 1988) p. 482.
28. S. V. NAIR and M. L. SHIAO, Communication Report to Monsanto Chemical Company.
29. R. T. DEHOFF, in "Encyclopedia of Materials Science and Engineering", Vol. 6, edited by M. B. Bever (MIT Press, Cambridge, MA, 1986) p. 4633.
30. D. STAUFFER, in "Introduction to Percolation Theory" (Taylor and Francis, London, 1985).
31. K. MIYASAKA, K. WATANABE, E. JOJIMA, H. AIDA, M. SUMITA and K. ISHIKAWA, *J. Mater. Sci.* **17** (1982) 1610.
32. W. Y. HSU, W. G. HOLTJE and J. R. BARKLEY, *J. Mater. Sci. Lett.* **7** (1988) 459.
33. G. J. HOWARD and R. A. SHANKS, *J. Macromol. Sci. Phys.* **B19** (1981) 167.
34. A. M. CHATTERJEE, F. P. PRICE and S. NEWMAN, *J. Polym. Sci. Polym. Phys.* **13** (1975) 2369.
35. D. CAMPBELL and M. M. QAYYUM, *ibid.* **18** (1980) 83.
36. J. L. THOMASON and A. A. VAN ROOYEN, *J. Mater. Sci.* **27** (1992) 897.
37. S. Y. HOBBS, *Nature Phys. Sci.* **234** (1971) 12.
38. P. D. FRAYER and J. B. LANDO, *J. Polym. Sci. B Polym. Lett.* **10** (1972) 29.
39. A. MISRA, B. L. DEOPURA, S. F. XAVIER, F. D. HARTLEY and R. H. PETERS, *Angew. Makromol. Chem.* **13** (1983) 113.
40. B. MAXWELL, *J. Polym. Sci.* **C9** (1965) 43.

Received 27 August 1992
and accepted 27 September 1993